International Journal of Engineering Research and Science & Technology

www.ijerst.org

ISSN : 2319-5991

Vol. 22 No. 4 (2026)



ijerst.editor@gmail.com

editor@ijerst.com

ISSN 2319-5991 www.ijerst.com
© 2026 IJERST. All Rights Reserved
Peer Reviewed, Referred & Indexed Journal

Research Paper

A THREE-STAGE SLOTTED HEXAGRAM MICROSTRIP PATCH ANTENNA DESIGN AND S-PARAMETER ANALYSIS FOR K-BAND AND 5G N258 APPLICATIONS

Authors Of This Project		Project Guide
Guddathahalli Mahammad Afshan[1]	Shaik Aaliya[2]	M. Anitha[7], Assistant Professor, Dept. of ECE, RGUKT RK Valley manitha@rguktrkv.ac.in
Chinnarangappagari Yasaswini[3]	Tunga Karuna Pradeep[4]	
Kammari Lokesh Achari[5]	Ulebeedu Ediga Harshavardhan Goud[6]	

Rajiv Gandhi University of Knowledge Technologies (RGUKT), RK Valley
Idupulapaya, Kadapa District, Andhra Pradesh – 516330, India

ABSTRACT—This paper presents a simulation-based study of a three-stage slotted hexagram microstrip patch antenna intended for 24 GHz K-band and millimeter-wave applications. A six-pointed-star (hexagram) patch on a 40 mm × 40 mm FR4 substrate is fed by a 3 mm microstrip line and analyzed in Ansys HFSS with a lumped port over a 2–30 GHz sweep. The geometry evolves from a solid hexagram (Stage 1), to a hexagram with six triangular arm slots (Stage 2), to a hexagram with six triangular arm slots and a central circular slot (Stage 3). The reported S_{11} minima are −11.8980 dB at 25.10 GHz, −12.8660 dB at 24.96 GHz, and −16.7466 dB at 24.60 GHz for Stages 1–3, respectively, i.e., a 500 MHz downward shift of the marked resonance and an S_{11} improvement of about 4.85 dB. The Stage 3 resonance lies within the 5G NR n258 range (24.25–27.50 GHz). S_{11}, VSWR, and a simulated gain pattern at the Stage 3 resonance are reported; impedance bandwidth, quantified gain, efficiency, and measurements remain future work.

Keywords—5G NR n258, HFSS, hexagram patch antenna, K-band, millimeter-wave antenna, microstrip patch antenna, return loss, S-parameters, slotted antenna.

I. INTRODUCTION

Microstrip patch antennas are widely used in wireless systems because they are low-profile, lightweight, inexpensive to fabricate, and compatible with planar integration. Their performance depends on the patch geometry, substrate permittivity and thickness, feed arrangement, and ground-plane design, and established references describe the trade-offs among matching, bandwidth, efficiency, and radiation [1]–[4].

Non-rectangular patches and deliberate geometric perturbations are often investigated to tune resonance and improve impedance matching. In hexagonal designs, ground-plane slots, asymmetric slots, and parasitic elements have been reported as ways to modify current paths and influence bandwidth, gain, and multiband behavior [5]–[7]. Related studies address hexagonal patches for UWB operation [8], CPW-fed IoT antennas [9], and circular polarization [10]. These works show that geometry and feeding must be assessed together, and they motivate examining a six-pointed-star (hexagram) patch with slot loading at higher frequencies.

The 24 GHz region of the K-band is of interest for short-range radar, vehicular sensing, and millimeter-wave communication; the 5G NR n258 band spans 24.25–27.50 GHz. This paper studies a three-stage evolution of a hexagram microstrip patch on FR4 and compares the simulated reflection coefficient of a solid hexagram, a hexagram with six triangular arm slots, and a hexagram with the same slots plus a central circular slot. The study centers on the simulated S_{11} of all three stages, supplemented by the VSWR and a gain pattern for Stage 3; impedance bandwidth, quantified gain, efficiency, and measured results are listed as future work.

II. ANTENNA CONFIGURATION AND DESIGN METHODOLOGY

A. Substrate and Material Specifications

The antenna is built on an FR4 epoxy substrate (ε_r = 4.4, μ_r = 1.0, tan δ = 0.02, density 1900 kg/m³) measuring 40 mm × 40 mm with a thickness of 1.5 mm. At 24.60 GHz the free-space wavelength is $\lambda_0 \approx 12.19$ mm, so h = 1.5 mm corresponds to $\approx 0.12\ \lambda_0$, which is electrically thick for a microstrip substrate and may increase surface-wave and feed radiation effects. The relatively high loss tangent of FR4 at millimeter-wave frequencies is also expected to limit radiation

efficiency, which has not yet been evaluated. Material and dimension data are summarized in Table I.

TABLE I
ANTENNA DESIGN AND MATERIAL PARAMETERS

Parameter	Value
Substrate material	FR4 epoxy
Relative permittivity, ε_r	4.4
Relative permeability, μ_r	1.0
Loss tangent, tan δ	0.02
Mass density	1900 kg/m³
Substrate length × width	40 mm × 40 mm
Substrate thickness, *h*	1.5 mm
Ground plane	Copper, 40 mm × 40 mm
Feed line	Microstrip, width 3 mm
Feed–patch transition	Angled

B. Antenna Geometry

The hexagram has an outer radius of approximately 11 mm and an inner radius of approximately 6.4 mm. Each triangular slot has a base of approximately 2 mm and a height of approximately 3.5 mm, the central circular slot has a diameter of approximately 6 mm, and the 3 mm wide feed line is approximately 9 mm long.

C. Feeding Mechanism

The patch is excited by a 3 mm wide microstrip line connected to the hexagram through an angled transition, and the line is intended to present a 50 Ω characteristic impedance. As a plausibility check only, the quasi-static microstrip expressions in [2], [4] give approximately 49 Ω for a 3 mm line on a 1.5 mm FR4 substrate (εr = 4.4), neglecting conductor thickness and dispersion, which is consistent with the intended 50 Ω design value.

D. HFSS Simulation Setup

The antenna was simulated in Ansys HFSS using a lumped-port excitation with a 50 Ω reference impedance, a radiation boundary, and a frequency sweep from 2 GHz to 30 GHz. The radiation air box is 60 mm × 60 mm × 8 mm. Table II lists the setup. The copper ground plane is specified as 40 mm × 40 mm on the bottom substrate surface.

TABLE II
HFSS SIMULATION PARAMETERS

HFSS setting	Value
Software	Ansys HFSS
Frequency sweep	2 GHz to 30 GHz
Sweep type / step size	Fast sweep, 2–30 GHz
Excitation	Lumped port, 50 Ω reference
Port sheet position (x, y, z)	(−20, −1.5, 0) mm
Port sheet size	3 mm × 1.5 mm
Integration line	Vertical (along z), from ground plane to feed line
Boundary	Radiation
Air box (X × Y × Z)	60 mm × 60 mm × 8 mm
Output	S_{11} (dB)

E. Performance Parameters

The reflection coefficient at the antenna input is

$$\Gamma = \frac{Z_{in}-Z_0}{Z_{in}+Z_0} \quad (1)$$

where Z_{in} is the input impedance and Z_0 = 50 Ω is the reference impedance. The simulated S_{11} in decibels and the return loss are

$$S_{11}(dB) = 20log_{10}|\Gamma| \quad (2)$$

The resonant frequency is inversely related to the effective electrical length of the current path,

$$f_r \propto \frac{1}{L_{eff}} \quad (3)$$

where L_{eff} is the effective electrical length. A practical matching criterion is $S_{11} \leq -10$ dB, equivalent to $|\Gamma| \approx 0.316$, VSWR ≈ 1.93, and about 10% of the incident power reflected (90% accepted). The reflected power fraction is $|\Gamma|^2$, i.e., 10 raised to the power $S_{11}/10$ with S_{11} in dB, which is applied to the reported S_{11} values in Section IV-F.

III. THREE-STAGE ANTENNA DESIGN EVOLUTION

A. Stage 1: Solid Hexagram Patch

Stage 1 is a solid six-pointed-star metallic patch without slots, connected to the feed line through an angled transition (Fig. 1). It is the baseline antenna.

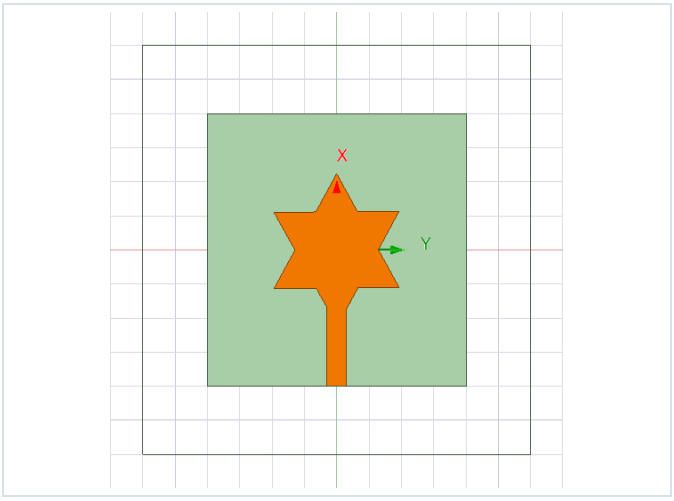


Fig. 1. Stage 1 solid hexagram antenna geometry (HFSS top view).

B. Stage 2: Hexagram Patch with Six Triangular Slots

Stage 2 introduces six symmetrical triangular slots, one in each star arm, while retaining the overall hexagram outline (Fig. 2). Removing metal from the arms is expected to perturb the current paths and the input impedance; this expectation is not yet supported by HFSS surface-current plots.

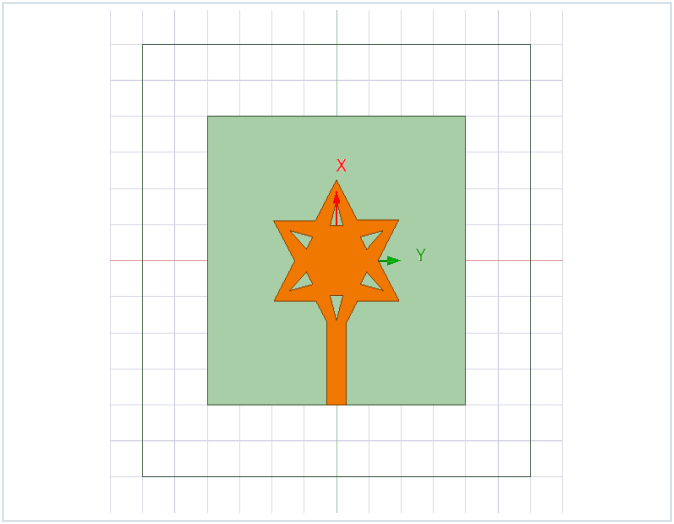


Fig. 2. Stage 2 hexagram antenna geometry with six triangular arm slots (HFSS top view).

C. Stage 3: Slotted Hexagram with Central Circular Slot

Stage 3 keeps the six triangular arm slots and adds a circular slot in the central region, giving a centrally apertured, slotted hexagram patch (Fig. 3). The downward resonance shift with added slots is consistent with a longer effective current path, but this interpretation requires surface-current evidence before it can be asserted.

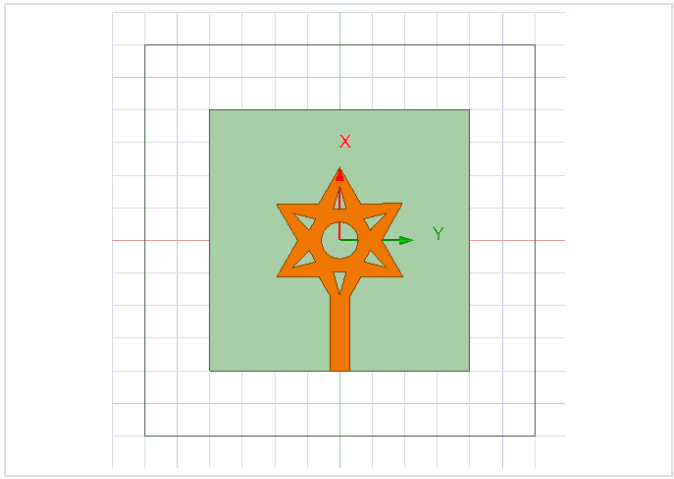


Fig. 3. Stage 3 slotted hexagram antenna geometry with central circular slot (HFSS top view).

IV. SIMULATION RESULTS AND DISCUSSION

The values below are the HFSS-marked minima of the simulated S_{11} curves. Resonance is identified here as the S_{11} minimum; it is not by itself a demonstration of usable operating bandwidth.

A. Stage 1 S_{11} Analysis

The Stage 1 response has a selected marker (m1) at 25.1000 GHz, where $S_{11} = -11.8980$ dB (Fig. 4). A second marker (m2) indicates $S_{11} = -11.8708$ dB at 25.1700 GHz. The response continues to decrease toward the upper sweep limit, reaching approximately −13.4 dB near 30 GHz. Therefore, the selected marker at 25.10 GHz should not be interpreted as the global minimum over the complete 2–30 GHz sweep. Further frequency-sweep analysis is required to identify all resonant regions.

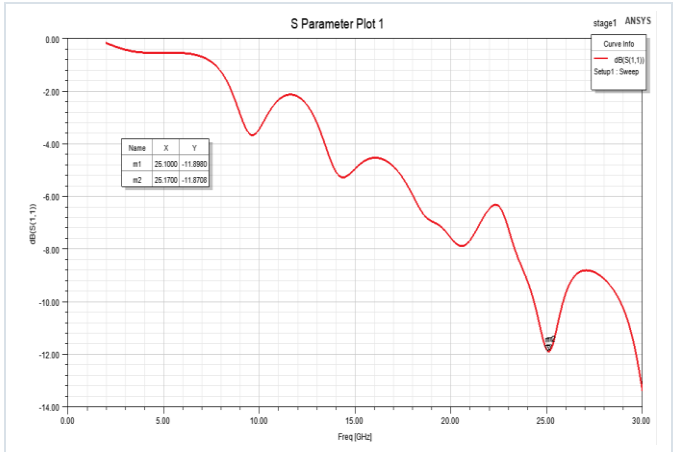


Fig. 4. Simulated S_{11} response of Stage 1.

B. Stage 2 S_{11} Analysis

Stage 2 shows its marked minimum at 24.9600 GHz with $S_{11} = -12.8660$ dB (Fig. 5). Relative to Stage 1, this is a 140 MHz downward shift and a 0.968 dB deeper minimum, so adding the six triangular arm slots slightly lowers the resonant frequency and improves the match. About 5.17% of the incident power is reflected at this minimum, compared with 6.46% for Stage 1 (Table V).

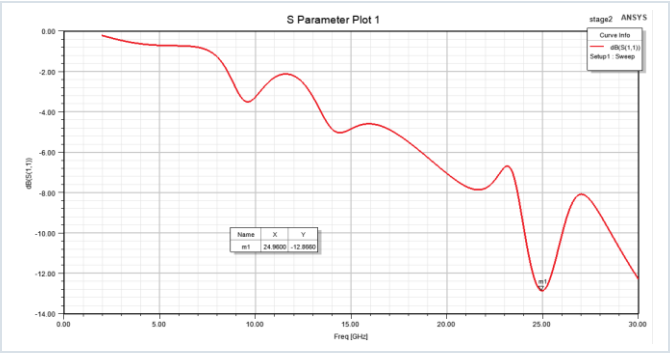


Fig. 5. Simulated S_{11} response of Stage 2.

C. Stage 3 S_{11} Analysis

Stage 3 shows a pronounced, narrow minimum at 24.6000 GHz with S_{11} = −16.7466 dB (Fig. 6). A shallower, unmarked dip of roughly −9.7 dB is visible near 20.5 GHz (read from the plot), which does not reach the −10 dB criterion.

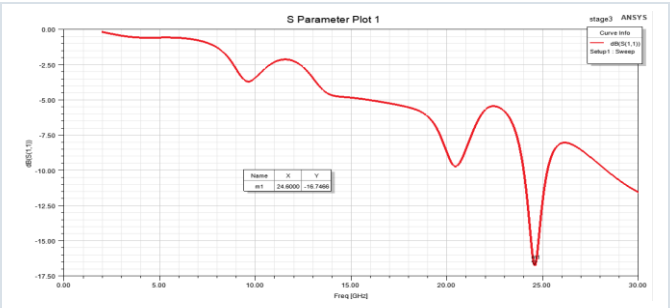


Fig. 6. Simulated S_{11} response of Stage 3.

D. Comparative Analysis

Table III and Fig. 7 compare the three stages. The curves coincide closely below about 14 GHz and diverge mainly in the 18–30 GHz region, where the slot loading changes the response.

TABLE III
THREE-STAGE ANTENNA PERFORMANCE COMPARISON

Stage	Configuration	Frequency	S_{11}
Stage 1	Solid Hexagram	25.10 GHz	−11.8980 dB
Stage 2	Triangular Arm Slots	24.96 GHz	−12.8660 dB
Stage 3	**Triangular and Circular Slots**	**24.60 GHz**	**−16.7466 dB**

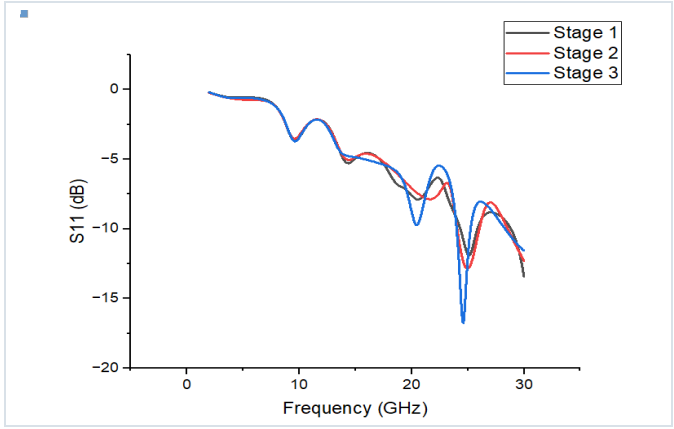


Fig. 7. Combined simulated S_{11} comparison of the three antenna stages.

E. Resonant Frequency Shift

The marked resonance moves downward from 25.10 GHz (Stage 1) to 24.96 GHz (Stage 2) and 24.60 GHz (Stage 3), a total shift of 500 MHz (≈ 1.99%). The larger step (360 MHz) occurs with the central circular slot (Table IV). Without surface-current data, the mechanism is not established.

TABLE IV
RESONANT FREQUENCY SHIFT AND S_{11} CHANGE

Transition	Δf_r (MHz)	ΔS_{11} (dB)	$\Delta f_r/f_r$ (%)
Stage 1 → 2	−140	-0.9680	-0.56
Stage 2 → 3	−360	-3.8806	-1.44
Stage 1 → 3	−500	-4.8486	-1.99

F. Impedance Matching Improvement

S_{11} improves from −11.8980 dB to −16.7466 dB, a total change of about 4.85 dB, with Stage 3 giving the best reported match. Table V converts the reported values using (1)–(3) with Z_0 = 50 Ω. Stage 3 reflects about 2.12% of the incident power (VSWR ≈ 1.34), compared with about 6.46% (VSWR ≈ 1.68) for Stage 1. All three stages satisfy the −10 dB criterion at their marked minima, but Stages 1 and 2 do so with limited margin. The −10 dB impedance bandwidth has not been extracted from the simulated data and is left for future work.

TABLE V
DERIVED REFLECTION METRICS FROM REPORTED S_{11}

Stage	$\lvert\Gamma\rvert$	RL (dB)	VSWR	P_{refl} (%)	$P_{accepted}$ (%)
1	0.2542	11.8980	1.682	6.46	93.54
2	0.2274	12.8660	1.589	5.17	94.83
3	**0.1454**	**16.7466**	**1.340**	**2.12**	**97.88**

G. VSWR Analysis

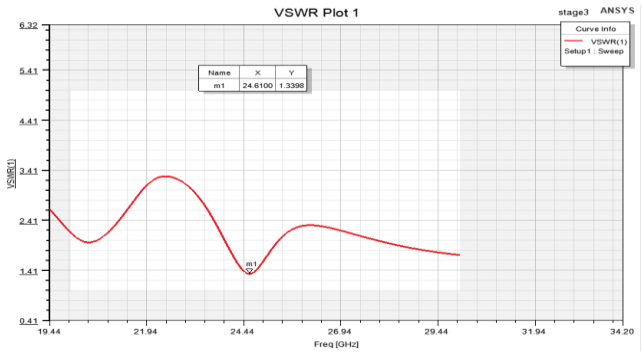


Fig.8 . Simulated VSWR response of the Stage 3 antenna.

Away from the resonance the VSWR rises above 2 (about 3.3 near 22 GHz), although it falls again to about 1.7 near the 30 GHz sweep limit. The match near 24.6 GHz is therefore narrow, and the upper band edge needs a wider sweep..At the marked resonance of 24.61 GHz the VSWR is 1.34, which agrees with the value derived from the reported S_{11} in Table V and is well below the value of 1.93 that corresponds to $S_{11} = -10$ dB. A VSWR close to 1 indicates a good impedance match to the 50 Ω feed at this frequency. Fig. 8 shows the simulated VSWR of the Stage 3 antenna.

H. Radiation Pattern

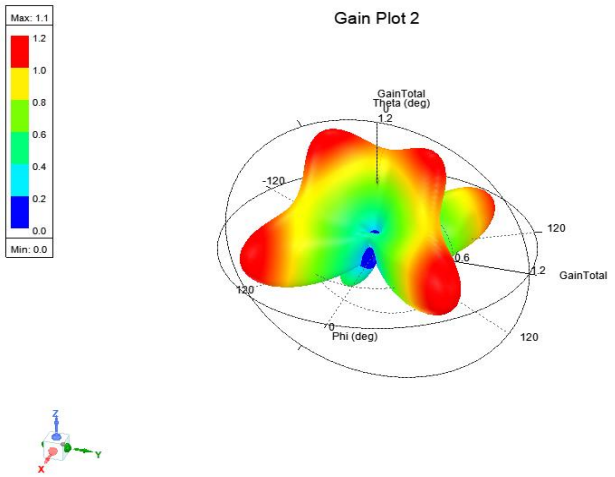


Fig. 9. Simulated 3D gain pattern of the Stage 3 antenna at 24.6 GHz.

Fig. 9 shows the simulated three-dimensional total gain pattern of the Stage 3 antenna at the resonant frequency of 24.6 GHz. The colour scale represents the gain magnitude, with red regions indicating the highest gain and blue regions the lowest. The pattern is multi-lobed rather than a single broadside beam, and the maximum gain on the plot scale is about 1.1 (linear), which corresponds to roughly 0.4 dBi. A possible contributor is the high loss tangent of FR4 at millimeter-wave frequencies, although efficiency has not been evaluated. The irregular lobe structure may be related to the slotted hexagram geometry and the electrically thick substrate; this interpretation is not yet supported by surface-current data, and a detailed study of the radiation characteristics is left for future work.

V. POTENTIAL APPLICATIONS

The Stage 3 resonance at 24.60 GHz lies within the 5G NR n258 range (24.25–27.50 GHz); the Stage 1 and Stage 2 resonances (25.10 GHz and 24.96 GHz) also fall in this range. None of the three resonances lies within the 24.0–24.25 GHz ISM allocation. The design is therefore a candidate for 5G millimeter-wave communication and wireless backhaul, and could be explored for short-range radar, vehicular sensing, and other high-frequency wireless systems if the operating band is adjusted or shown to cover the required frequencies. Regulatory allocations differ by region, and suitability for any application additionally requires demonstrated impedance bandwidth, quantified gain, and efficiency, which are not reported here.

VI. FUTURE WORK

The following are required to strengthen the study and are not part of the present results:

1) Quantified peak realized gain, directivity, and 2D radiation patterns (E- and H-plane cuts).
2) −10 dB impedance bandwidth from exported S_{11} data.
3) Surface-current and electric-field distributions to support the slot-loading interpretation.
4) Fabrication and VNA measurement, with comparison to simulation.
5) Parametric optimization of the slot dimensions toward deeper matching.

VII. CONCLUSION

A three-stage slotted hexagram microstrip patch antenna was simulated in HFSS for K-band and 5G n258 applications. Adding six triangular arm slots and a central circular slot to a solid hexagram moved the marked resonance from 25.10 GHz to 24.60 GHz and improved the simulated S_{11} from −11.8980 dB to −16.7466 dB, the best reported match being Stage 3. These conclusions rest mainly on simulated S_{11} and VSWR; impedance bandwidth, quantified gain, efficiency, and measured validation are still needed.

REFERENCES

[1] C. A. Balanis, *Antenna Theory: Analysis and Design*, 4th ed. Hoboken, NJ, USA: Wiley, 2016.
[2] D. M. Pozar, *Microwave Engineering*, 4th ed. Hoboken, NJ, USA: Wiley, 2011.
[3] K. R. Carver and J. W. Mink, “Microstrip antenna technology,” *IEEE Trans. Antennas Propag.*, vol. 29, no. 1, pp. 2–24, Jan. 1981, doi: 10.1109/TAP.1981.1142523.

[4] R. Garg, P. Bhartia, I. Bahl, and A. Ittipiboon, *Microstrip Antenna Design Handbook*. Norwood, MA, USA: Artech House, 2001.

[5] N. Kushwaha and R. Kumar, "Design of slotted ground hexagonal microstrip patch antenna and gain improvement with FSS screen," *Prog. Electromagn. Res. B*, vol. 51, pp. 177–199, 2013, doi: 10.2528/PIERB13031604.

[6] R. V. S. R. Krishna, R. Kumar, and N. Kushwaha, "Design of asymmetrically slotted hexagonal patch antenna for high-gain UWB applications," *Int. J. Microw. Wireless Technol.*, vol. 7, no. 5, pp. 571–577, 2015, doi: 10.1017/S1759078714000865.

[7] K. Mandal and P. P. Sarkar, "A compact high gain microstrip antenna for wireless applications," *AEU – Int. J. Electron. Commun.*, vol. 67, no. 12, pp. 1010–1014, 2013, doi: 10.1016/j.aeue.2013.06.001.

[8] K. Singh, S. Patil, A. Naik, and S. Kadam, "Hexagonal microstrip patch antenna design for UWB application," *ITM Web Conf.*, vol. 44, Art. no. 02004, 2022, doi: 10.1051/itmconf/20224402004.

[9] R. Devi and S. K. Prasad, "A hexagonal slotted CPW-fed antenna with parasitic patch for Internet of Things applications," in *Proc. 2022 URSI Reg. Conf. Radio Sci. (URSI-RCRS)*, Indore, India, Dec. 2022, pp. 1–4.

[10] K. Joshi, D. Yadav, and D. Bhardwaj, "Design of coplanar proximity coupled feed hexagonal shaped circular polarized microstrip patch antenna," *Trends Sci.*, vol. 19, no. 18, p. 4170, 2022, doi: 10.48048/tis.2022.4170.